

Graphical Abstract

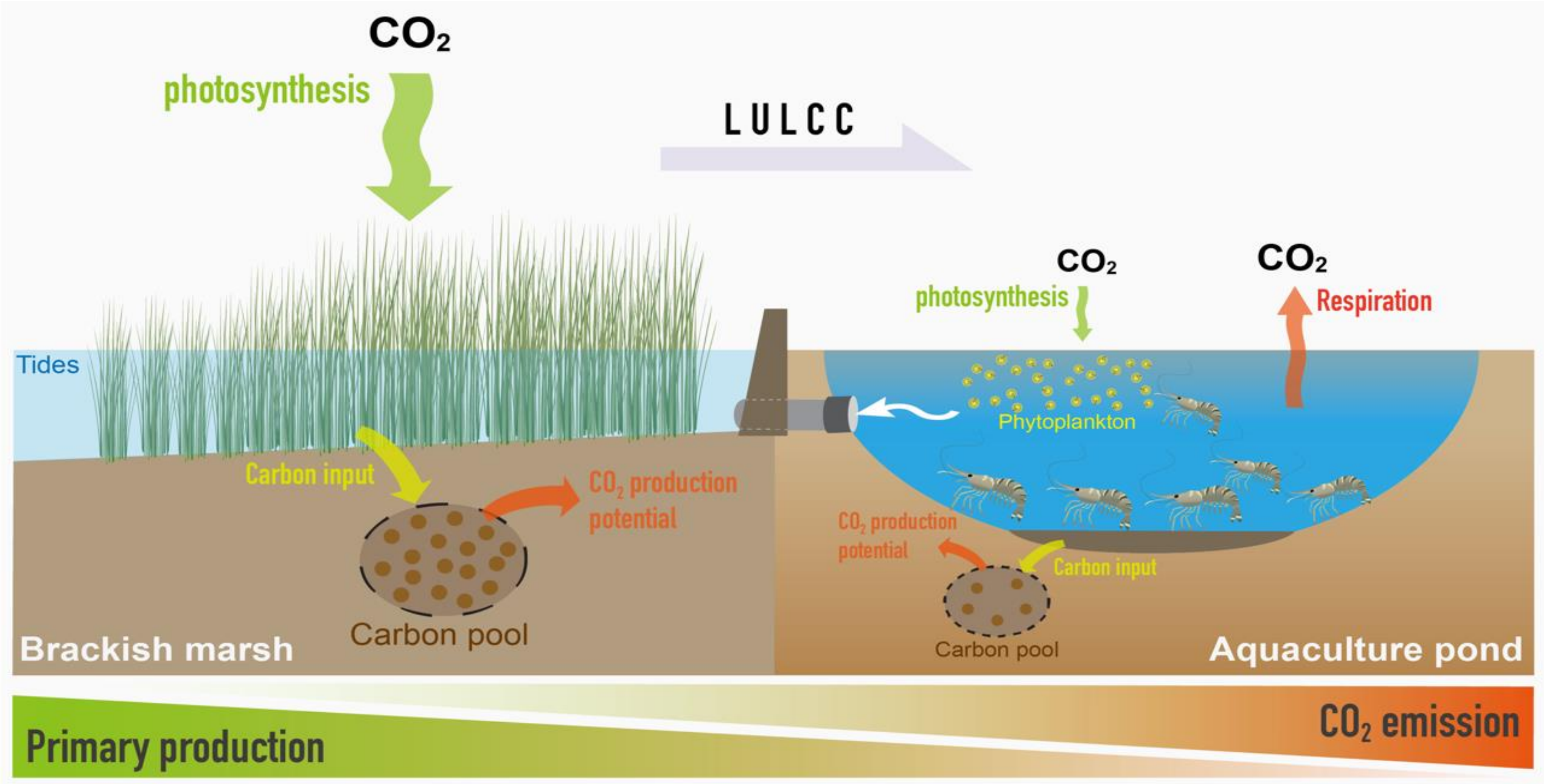

HIGHLIGHTS

- Converting coastal marsh to aquaculture ponds increased CO_2 emission by 101%
- Sediment anaerobic CO_2 production potential decreased by 69% after conversion
- Marsh vegetation played a key role in CO_2 uptake and sequestration
- Sediment temperature was a main physical driver in CO_2 seasonal dynamics

Effects of conversion of coastal marshes to aquaculture ponds on sediment anaerobic CO_2 production and emission in a subtropical estuary of China

Lishan Tan[a,b], Linhai Zhang[a,b], Ping Yang[a,b,c,d*], Chuan Tong[a,b,d], Derrick Y.F. Lai[e], Hong Yang[f,g], Yan Hong[a], Yalan Tian[a], Chen Tang[a], Manjing Ruan[a], Kam W. Tang[h*]

[a]*School of Geographical Sciences, Fujian Normal University, Fuzhou 350117, P.R. China*

[b]*Institute of Geography, Fujian Normal University, Fuzhou 350117, P.R. China*

[c]*Fujian Provincial Key Laboratory for Subtropical Resources and Environment, Fujian Normal University, Fuzhou 350117, P.R. China*

[d]*Key Laboratory of Humid Subtropical Eco-geographical Process of Ministry of Education, Fujian Normal University, Fuzhou 350117, P.R. China*

[e]*Department of Geography and Resource Management, The Chinese University of Hong Kong, Hong Kong, China*

[f]*College of Environmental Science and Engineering, Fujian Normal University, Fuzhou 350007, P.R. China*

[g]*Department of Geography and Environmental Science, University of Reading, Reading, RG6 6AB, UK*

[h]*Department of Biosciences, Swansea University, Swansea SA2 8PP, U. K.*

***Correspondence to:**

Ping Yang (yangping528@sina.cn); Kam W. Tang (k.w.tang@swansea.ac.uk)

Telephone: 086-0591-87445659 **Fax:** 086-0591-83465397

A B S T R A C T

The extensive conversion of carbon-rich coastal wetland to aquaculture ponds in the Asian Pacific region has caused significant changes to the sediment properties and carbon cycling. Using field sampling and incubation experiments, the sediment anaerobic CO_2 production and CO_2 emission flux were compared between a brackish marsh and the nearby constructed aquaculture ponds in the Min River Estuary in southeastern China over a three-year period. Marsh sediment had a higher total carbon and lower C:N ratio than aquaculture pond sediment, suggesting the importance of marsh vegetation in supplying labile organic carbon to the sediment. Conversion to aquaculture ponds significantly decreased sediment anaerobic CO_2 production rates by 69.2% compared to the brackish marsh, but increased CO_2 emission, turning the CO_2 sink (-490.8 ± 42.0 mg m^{-2} h^{-1} in brackish marsh) into a source (6.2 ± 3.9 mg m^{-2} h^{-1} in aquaculture pond). Clipping the marsh vegetation resulted in the highest CO_2 emission flux (382.6 ± 46.7 mg m^{-2} h^{-1}), highlighting the critical role of marsh vegetation in capturing and sequestering carbon. Sediment anaerobic CO_2 production and CO_2 uptake (in brackish marsh) and emission (in aquaculture ponds) were highest in the summer, followed by autumn, spring and winter. Redundancy analysis and structural equation modeling showed that the changes of sediment temperature, salinity and total carbon content accounted for more than 50% of the variance in CO_2 production and emission. Overall, the results indicate that vegetation clearing was the main cause of change in CO_2 production and emission in the land conversion, and marsh replantation should be a

primary strategy to mitigate the climate impact of the aquaculture sector.

Keywords: Organic carbon decomposition; Carbon dioxide (CO_2) fluxes; Habitat alteration; Coastal wetland; Aquaculture ponds

1. Introduction

Global climate change due to increased emission of greenhouse gases (GHGs) is one of the most pressing environmental issues of our time. Carbon dioxide (CO_2) accounts for nearly 60% of the total atmospheric radiative forcing (IPCC, 2014; Le Quéré et al., 2018). In 2021, the atmospheric CO_2 concentration reached a new peak value of 415.7 ppm. (World Meteorological Organization, 2022). Despite the small areal coverage of marine vegetated habitats such as salt marshes, mangroves and seagrass beds— about 0.2% of the ocean surface, they have disproportionate influence on the global carbon cycle, contributing ~50% of the annual carbon burial into the sediment (Duarte et al., 2013). Due to the high primary productivity and organic matter burial and anaerobic soil condition, coastal wetlands sequester atmospheric CO_2 at a rate ≥ 10 times higher than terrestrial forests (Mcleod et al., 2011; Mitsch et al., 2013; Tan et al., 2020). As such, even small disturbances to these coastal habitats may have a strong feedback on global carbon emission and climate warming (IPCC, 2014; Yao et al., 2021).

Land-use and land-cover change (LULCC) is now the second largest anthropogenic cause of GHG emissions, trailing only fossil fuel combustion (Friedlingstein et al., 2020; IPCC, 2014). More than 16% of the coastal wetlands around the globe have been impacted by LULCC (Hong et al., 2021; Murray et al., 2019), with an estimated annual loss rate of 0.2–5.0 % (Davidson and Finlayson, 2019). Along with a rapidly growing population, aquaculture plays a significant role in improving nutritional status and food security, promoting ocean and marine resource sustainability and socioeconomic development, all of which can help achieve the 2030 United Nations Sustainable Development goals (Ottinger et al., 2016; Suweis et al., 2015). In China, more than 11,163 km^2 of the natural coastal wetlands has been cleared for development since the 1950s, most of which was for the construction of earthen aquaculture ponds (Meng et al., 2017; Ren et al., 2019). The total area of aquaculture ponds converted from coastal wetlands in China was approximately 8,629 km^2 in 2021 (Duan et al., 2021; Wang et al., 2023).

This extensive habitat transformation removes the vegetation and converts free-flowing water to standing water (He et al., 2021; Yang et al., 2022a), and the addition of animal wastes and excess feeds from aquaculture is expected to enhance carbon mineralization in the sediment (Naskar et al., 2020; Ye et al., 2022). Within the anoxic, organic-rich sediment, microbial production of methane (CH_4) is a main concern due to its high warming potential (Beaulieu et al., 2019; Sepulveda-Jauregui et al., 2018). Studies have shown that converted aquaculture ponds have higher CH_4 emission than the natural wetlands (Tan et al., 2020; Yang et al., 2022a), which could be partly explained by an increase in ebullition as the main CH_4 transport pathway (Yang et al., 2022a). In inundated sediment, CO_2 production by anaerobic respiration using various electron acceptors usually precedes methanogenesis along the Redox cascade (Gruca-Rokosz et al., 2011; Xing et al., 2005). Indeed, CO_2 efflux from sediment is estimated to be orders of magnitude higher than CH_4 efflux in eutrophic inland habitats (Gruca-Rokosz and Tomaszek, 2015; Xing et al., 2005) and coastal wetlands (Barroso et al., 2022; Hsieh et al., 2021; Magenheimer et al., 1996). Unlike CH_4, the transport of the highly soluble CO_2 is primarily through diffusion rather than ebullition, and it can be recaptured by photoautotrophs, possibly leading to uncoupling between sediment CO_2 production and net emission to air.

As earthen pond aquaculture continues to expand and intensify along the coast of China (Duan et al., 2021; Ren et al. 2019; Yang et al., 2022b) and elsewhere in SE Asia (Luo et al., 2022), it is necessary to investigate the effects of LULCC on sediment CO_2 production and emission in coastal wetlands over a longer period and in a higher temporal resolution. Such data will help scientists estimate more accurately the CO_2 budget and emission in impacted wetlands, and the feedback on climate along the rapidly changing coastal landscape (Hopkinson et al., 2012; Pendleton et al., 2012). Ideally, one should monitor the change throughout the process of land conversion. Unfortunately, historical environmental data and routine monitoring is lacking for many of the converted aquaculture ponds. To circumvent this problem, in this study we compared the sediment anaerobic CO_2 production, CO_2 emission fluxes and associated physicochemical factors between a brackish marsh and an area that had been converted to aquaculture ponds, in the Min River estuary of southeastern China, with high-frequency sampling over a three-year period. To gain an insight into the effect of vegetation clearing—a standard practice when constructing earthen ponds—on CO_2 emission, we included a treatment where we clipped the aboveground shoots in the marsh. We aimed to evaluate the effects of converting coastal marshes to aquaculture ponds on sediment CO_2 production and emission, and to identify key physicochemical factors that drive the response of CO_2 to land conversion.

2. Materials and methods

2.1. Study area

The Shanyutan wetland (26°00′36″ to 26°03′42″N, 119°34′12″ to 119°40′40″E) in the Min River estuary, Fujian, in southeastern China (Figure 1) is influenced by a subtropical monsoonal climate, with a mean annual air temperature of ca. 19.6 °C and a mean annual precipitation of 139 cm (Yang et al., 2022a). Salt water of 4.2±2.5 ‰ average salinity 0inundates the wetland via semidiurnal tides of 2.5–6.0 m (Tong et al., 2018). The dominant vegetation here includes the native *Cyperus malaccensis* and *Phragmites australis*, and the invasive *Spartina alterniflora*. Over the past decades, extensive areas of *C. malaccensis* and *S. alterniflora* marshes have been converted to earthen aquaculture ponds for food production, mostly shrimp (*Litopenaeus vannamei*) (Yang et al., 2022b).

The size of the aquaculture ponds in the region ranges from 1.2 to 3.0 ha, with a mean water depth of ~1.5 m. The period of shrimp farming is from June to November and the stocking density is 150–250 postlarvae m^{-2}. The shrimp are fed pellets (5000 kg ha^{-1}) daily at 08:00 a.m. and 4:00 p.m. local time. There is no water exchange during the farming period (Yang et al., 2022b).

A brackish *C. malaccensis* marsh and three converted aquaculture ponds nearby were selected for the study (Figure 1). Between April 2019 and January 2020, sampling and incubation experiments were carried out monthly for a total 10 times. Subject to Covid-19-related travel restrictions and staff availability, CO_2 fluxes from the brackish marsh and aquaculture ponds were measured between April 2019 and December 2021 for a total of 36 times during the three-year period.

2.2. Collection and analysis of sediment

Three permanent quadrats (1 m × 1 m) two meters apart were established within *C. malaccensis* marsh for the collection of sediment and porewater samples. 15-cm long sediment cores were collected in each quadrat using a steel cylinder (5 cm in diameter). For the aquaculture ponds, triplicate 15-cm long sediment cores were randomly collected within each pond. Sediment samples were stored at 4 ℃ in the dark until analysis. During each sampling campaign, sediment temperature (T_S) and electrical conductivity (EC) were measured *in situ* using a portable meter (2265FS, Spectrum Technologies, USA).

In the laboratory, sediment pH (sediment-to-water ratio of 1:2.5 w/v) and salinity (sediment-to-water ratio of 1:5 w/v) were measured with a pH meter (Orion 868, USA) and a salinity meter (Eutech Instruments- Salt6, USA), respectively. A subsample of the sediment was freeze-dried and ground in a ball mill after the removal of plant roots for the measurement of sediment total carbon (STC) and sediment total nitrogen (STN), using an elemental analyser (Elementar Vario MAX CN, Germany).

2.3. Collection and analysis of sediment porewater

To collect porewater from the marsh sediment, a series of PVC porewater samplers (5 cm inner diameter) were installed within each aforementioned quadrat in the marsh; each sampler extended 15 cm into the sediment and 5 cm above the sediment surface, with the top opening covered by a 0.2-μm nylon membrane screen (BiotransTM) (Tong et al., 2018).

To collect porewater from the aquaculture pond sediment, 15-cm long sediment cores were collected at three randomly sites in each pond using a steel cylinder sampler (5 cm inner diameter); the sediment porewater was then extracted by centrifugation at 4,000 rpm for 10 min (Hereaus Omnifuge 2000 RS) (Matos et al., 2016).

Approximately 50 mL of each porewater sample was filtered through a 0.45-μm filter (Biotrans™ nylon membranes) within 24 h of collection. The filtrates were stored at 4 ºC for further measurement within one week. Each porewater filtrate was split into four portions for measuring SO_4^{2-}, Cl^-, NH_4^+-N and NO_3^--N. SO_4^{2-} and Cl^- concentrations were measured with a Dionex 2100 ion chromatograph (Thermo Fisher Scientific, Sunnyvale, California, USA); NH_4^+-N and NO_3^--N concentrations were measured with a flow injection analyzer (Skalar Analytical SAN^{++}, Netherlands).

2.4. Measurement of sediment anaerobic CO_2 production

The sediment anaerobic CO_2 production was determined by incubation according to Liu et al. (2019) and Wang et al. (2017). Approximately 50 g of fresh sediment and 50 mL of *in situ* water were added to a 200-mL incubation bottle; the slurry was then purged with N_2 gas for 5–8 min to displace the oxygen. The bottles were sealed with a silicone rubber stopper and incubated at *in situ* sediment temperature with agitation (175 rpm) for 12 days. 5 mL of headspace sample was extracted from each incubation bottle every four days to measure CO_2 (total 4 times); 5 mL of N_2 gas was added back to balance the pressure. CO_2 concentrations of the extracted gas samples were determined on a gas chromatograph (GC-2014, Shimadzu, Kyoto, Japan) equipped with a flame ionization detector (FID). Sediment anaerobic CO_2 production [μg CO_2 g^{-1} (dry weight) d^{-1}] was calculated from the linear rate of increase in headspace CO_2 concentration over time (Liu et al., 2019; Yang et al., 2022b).

2.5. CO_2 flux measurements

Repeated measurements of CO_2 fluxes were made between April 2019 and December 2021. Triplicate plots (1 m × 1 m) were set up in the marsh to measure CO_2 flux using static chambers (100 cm height × 35 cm width × 35 cm length) made of transparent plexiglass (Yuan et al., 2015; Tong et al., 2010). The top of each chamber had an electric fan installed inside to mix the headspace during measurements; a permanently installed bottom collar with a water-filled channel (30 cm height, 35 cm width, 35 cm length) was inserted 20 cm into the sediment. To assess the effect of marsh vegetation on CO_2 flux, we established additional plots nearby where the plant shoots were clipped and sealed with petroleum jelly to prevent gaseous exchange through the stems (Kelker and Chanton, 1997; Tong et al., 2012; Yang et al., 2022a).

In each aquaculture pond, CO_2 flux across the water-air interface was measured with a floating chamber (Natchimuthu et al., 2017). The floating chamber covering an area of 0.1 m^2 and a volume of 5.2 L was made from a polyethylene basin (plexiglas®) with an electric fan installed inside, and was fitted with Styrofoam on the side for floatation. We covered the outside of the floating chamber with reflective aluminum foil to minimize internal heating by sunlight.

During each sampling campaign, headspace samples from the chambers were drawn into aluminum-foil gas sample bags (Dalian Delin Gas Packing Co., Ltd., China) at 15-minute intervals over a 45-min period at each sampling site. CO_2 concentration of the collected gas samples were determined within 48 h on a gas chromatograph (GC-2014, Shimadzu, Kyoto, Japan) equipped with FID. The flux of CO_2 (mg CO_2 m^{-2} h^{-1}) was calculated from rate of increase in headspace CO_2 concentration over time; the results were then extrapolated to the annual cumulative CO_2 emission (*CE*) as:

$$CE = \sum MFi \times Di \times 24 \qquad \text{(Eq.1)}$$

where *MFi* is the CO_2 flux at the *i*th month of the year (mg CO_2 m^{-2} h^{-1}) and *Di* is the number of days in that month; CO_2 fluxes for unobserved months were estimated as the average fluxes of the observed months in the same season.

2.6. Statistical analysis

Differences in physicochemical factors (i.e., *T*s, sediment salinity, sediment pH, STC, STN, concentrations of SO_4^{2-}, Cl^-, NH_4^+-N and NO_3^--N in porewater), anaerobic CO_2 production and CO_2 fluxes between habitats (brackish marsh and aquaculture ponds) and between seasons were tested by one-way analysis of variance (ANOVA) using SPSS version 25.0 software (SPSS Inc., Chicago, IL, USA). The change rates of CO_2 production (ΔP_{CO2}), CO_2 fluxes (ΔF_{CO2}) and physicochemical factors (i.e., ΔTs, ΔSalinity, ΔpH, ΔSTC, ΔSTN, ΔSO_4^{2-}, ΔCl^-, ΔNH_4^+-N and ΔNO_3^--N) between the two habitats can reflect the synchronous responses of CO_2 dynamics and environmental factors to land conversion. Redundancy analysis (RDA) was performed to explore the relative influence of the change rates of different physicochemical factors on ΔP_{CO2} and ΔF_{CO2} using CANOCO 5.0 software (Microcomputer Power, Ithaca, NY, USA). To further examine the direct and indirect effect of the different physicochemical factors on ΔP_{CO2} and ΔF_{CO2}, a partial least square structural equation modeling (PLS-SEM) analysis was performed in R V3.5.3 (R

Foundation for Statistical Computing, 2013) with the 'semPLS' package. Briefly, the physicochemical factors were successively entered into the PLS-SEM in descending order by relative influence of each physicochemical factor from the RDA results, until the model cannot achieve significance. Then we test the PLS-SEM with different paths among the selected variables following a reasonable and conceptual assumption regarding variable dependencies, and the final model with the minimum Akaike's information criterion (AIC) was obtained. AIC was generally calculated for the simple regression model and the segmented linear regression model to assess fit of the models. Maximum-likelihood estimation was used to obtain the path coefficients, and the χ^2 goodness-of-fit test, degrees of freedom, p value (Chi-square) and AIC were used to evaluate the model (Šímová et al., 2019; Tan et al., 2022). All data were presented as mean ± standard error (SE), unless otherwise stated. In all statistical tests, a significance level of $p < 0.05$ was used.

3. Results

3.1. Physicochemical characteristics of sediment and porewater

The physicochemical characteristics of the sediments and porewaters are shown in Figure S1. The sediments in both habitats were brackish (mean salinity < 10‰) and slightly acidic (pH < 7). The porewater SO_4^{2-} and Cl^- concentrations were both lower than the typical values in seawater, and the average sediment C:N molar ratio was ~16 in the marsh and ~21 in the aquaculture ponds, substantially higher than the Redfield ratio.

Compared to the brackish marsh, the aquaculture ponds had significantly lower sediment T_S, salinity, STC and STN, as well as lower concentrations of porewater Cl^-, NO_3^-

-N and NH_4^+-N (p < 0.01 or < 0.05; Figures S1a, b, e, g and h), while the differences in sediment pH and porewater SO_4^{2-} concentration were insignificant (p > 0.05; Figures S1c, d, f and i).

3.2. Sediment anaerobic CO_2 production

The sediment anaerobic CO_2 production in the marsh averaged 606.7 ± 117.1 ug g^{-1} d^{-1} (range 116.4–990.9 ug g^{-1} d^{-1}), which was significantly higher than that in the aquaculture ponds (186.7 ± 38.2 ug g^{-1} d^{-1}; range 42.2–373.8 ug g^{-1} d^{-1}) (p < 0.01; Figure 2a). Both habitats showed the same seasonal differences in the sediment anaerobic CO_2 production, with significantly higher rates in the summer, followed by autumn, spring and winter (Figure 2b). The sediment carbon turnover rate, calculated as the ratio of anaerobic CO_2 production rate to STC, was 3% d^{-1} in the marsh and 1.2% d^{-1} in the aquaculture ponds.

3.3. CO_2 emission fluxes

The brackish marsh acted as a CO_2 sink during the whole study period, with the CO_2 flux ranging from -992.9 to -74.4 mg m^{-2} h^{-1} and averaging -490.8 ± 42.0 mg m^{-2} h^{-1} (Figure 3a). The net CO_2 uptake was highest in the summer, followed by autumn and winter, and lowest in spring (Figure 3c). Conversely, the clipped marsh acted as a strong source of CO_2 throughout the study; the CO_2 flux ranged from 35.6 to 1277.9 mg m^{-2} h^{-1} and averaged 382.6 ± 46.7 mg m^{-2} h^{-1} (Figure 3a), and was the highest in the summer (Figure 3d). The CO_2 flux from the aquaculture ponds varied between -19.0 and 77.9 mg m^{-2} h^{-1}, and it averaged 6.2 ± 3.9 mg m^{-2} h^{-1} (Figure 3b). The ponds acted as a CO_2 source in spring and summer, and as a sink in winter (Figure 3e).

Overall, the CO_2 flux was significantly different among the three habitats and was highest in the clipped marsh, followed by the aquaculture ponds, then the untreated marsh ($p < 0.05$). Extrapolating our measurements to a full year, the annual cumulative CO_2 flux from the marsh was -1037.7 to -2124.5 g CO_2 m^{-2} per year, whereas the aquaculture ponds emitted a total of -16.9 to 61.8 g CO_2 m^{-2} per year. In comparison, the clipped marsh released a total of 1015.3–1897.7 g CO_2 m^{-2} per year (Figure 4).

3.4. Environmental drivers of CO_2 production and flux

According to redundancy analysis (RDA), the environmental factors explained 75.5% of the variances in ΔF_{CO2} and ΔP_{CO2} among all data (Figure 5). Δsalinity, ΔT_S, ΔSTC and ΔCl^- together accounted for 80% relative influence (Figure 5). ΔT_S and ΔSTC were positively correlated with ΔF_{CO2} and ΔP_{CO2}, while Δsalinity and ΔCl^- were negatively correlated with ΔF_{CO2} and weakly to ΔP_{CO2}. Based on the structural equation model (SEM), ΔT_S had a direct positive effect on both ΔF_{CO2} and ΔP_{CO2}. ΔCl^- negatively affected ΔF_{CO2} directly and indirectly via ΔP_{CO2}. ΔSTC had a positive effect on ΔF_{CO2} by way of ΔP_{CO2} (Figure 6). Overall, ΔT_S had the largest total effect compared to ΔCl^- and ΔSTC (Figure 6).

We also conducted RDA and SEM analyses for the different habitats: The environmental factors explained 79.3% (marsh) and 76.8% (aquaculture ponds) of the variances in ΔF_{CO2} and ΔP_{CO2} (Figure S2). ΔCl^- had the largest relative influence in the marsh (61.4%), whereas in the aquaculture ponds it was ΔT_S (61.1%) (Figure S2). SEM analysis showed that ΔT_S had the largest total effect, negatively in the marsh and positively in the aquaculture ponds (Figure S3).

4. Discussion

The rapid growth and intensification of aquaculture worldwide has raised concerns of its environmental impacts including GHG emissions (Yuan et al., 2019). In China, the coastal land area converted for aquaculture use increased rapidly in the past three decades (Duan et al., 2021). To assess the related climate footprint, some researchers focused on GHG emissions due to feeds, fertilizers and energy consumption (Xu et al., 2022); others compared the aquaculture system types, cultivated species, environmental conditions and management practices (Bhattacharyya et al., 2013; Zhang et al., 2022). While those studies provide valuable information on the status quo of the aquaculture systems, they do not illustrate the systematic change in GHG dynamics caused by the land use change, especially for earthen aquaculture ponds that were constructed by clearing the coastal marshes.

Vegetated coastal wetlands play a key role in capturing and sequestering carbon into the sediment (Chmura et al., 2003; Duarte et al., 2013; Kirwan and Mudd, 2012). Based on our cumulative CO_2 flux estimates (Figure 4), the brackish marsh had an annual CO_2 uptake of 282–579 g C m^{-2} yr^{-1}, which is quite comparable to the estimated sediment carbon burial rate for coastal salt marshes in China (218 g C m^{-2} yr^{-1}; Meng et al., 2019). The conversion of a vegetated marsh to aquaculture ponds would remove this carbon burial capacity and also alter the sediment characteristics and GHG dynamics (Yang et al., 2022a, 2022c).

4.1. Effects of land use change on sediment and porewater characteristics

The aquaculture ponds were insulated from the tidal flushing by the warmer and saltier estuarine water, as reflected by the lower T_S, salinity and Cl^{-1} in the pond sediment and porewater relative to the marsh (Figure S1). Moreover, management practices often aim to maintain a stable physicochemical condition within the ponds to improve production. Despite the regular application of feeds and deposition of animal wastes, the pond sediment and porewater were less organic (STC, STN) and nutrient rich (NO_3^--N, NH_4^+-N) than the marsh (Figure S1), suggesting that tidal input and deposition by vegetation of organics and nutrients was more important in this ecosystem.

4.2. Effects of land use change on sediment anaerobic CO_2 production

The measured sediment anaerobic CO_2 production rate in the marsh sediment was > 2 times that in the aquaculture ponds (Figure 2). While SEM highlighted the strong effects of T_S and STC on sediment CO_2 production (Figure 6), T_S and STC differed by only 33% and 19%, respectively, between the marsh and the aquaculture ponds (Figure S1), and together they explained less than 40% of the variance in CO_2 production (Figure 5). Therefore, they were inadequate in explaining the difference in CO_2 production. Additionally, brackish marsh was supposed to have lower CO_2 production because higher sediment salinity may inhibit microbial metabolism (Chamber et al., 2013; Neubauer et al., 2013). However, salinity had only a weak influence on CO_2 production in SEM (Fig. 6). We speculate that the marsh vegetation released labile autochthonous organics and tidal flow also introduced more labile allochthonous organics into the marsh sediment, which together increased microbial respiration (Yang et al., 2022d). This is supported by the fact that the C:N ratio of the marsh sediment (~16) was lower than that of the aquaculture pond sediment (~21). The aquaculture operation may have also decreased sediment microbial diversity and microbial network complexity, resulting in lower overall microbial activity in the pond sediment (Yang et al., 2022c).

4.3. Effects of land use change on CO_2 flux

The marsh overall acted as a net CO_2 sink (Figure 3a) despite its high sediment CO_2 production rate (Figure 2). This suggests that carbon uptake by the marsh vegetation more than balanced the sediment CO_2 output, resulting in a net carbon burial (Duarte et al., 2013). The magnitude of this carbon sink was largest in the summer (Figure 3c), reflecting the higher photosynthetic activity due to the higher temperature and light intensity.

The important role of the vegetation in recycling the CO_2 from the sediment is further illustrated by the clipped marsh treatment: By clipping the above-ground biomass, the marsh became a strong CO_2 emitter (Figures 3a,d), likely fuelled by the high microbial CO_2 production, especially during the warmer months (Figure 2). Therefore, removal of marsh vegetation for the construction of aquaculture ponds may result in an initial surge of 873.4 mg CO_2 m^{-2} h^{-1} emission until the sediment carbon stock became depleted or removed.

The aquaculture ponds acted as a CO_2 emitter for much of the time (Figure 3b), especially in spring and summer when shrimp farming activity was the most intense (Figure 3e). Therefore, respiration by shrimp and microbes might significantly contribute to CO_2 emission. This is consistent with previous studies highlighting the GHG output from earthen aquaculture ponds (Yuan et al., 2019; Zhang et al., 2019). Based on the average CO_2 flux measurements, land use change from a marsh to aquaculture ponds would lead to a net increase of 497 mg CO_2 m^{-2} h^{-1} output from the land (in addition to the initial surge due to removal of vegetation, as discussed above). This is also consistent with previous studies showing that LULCC increases CO_2 emission (Kauffman et al., 2018; Sasmito et al., 2019; Tan et al., 2020).

A recent mesocosm study has shown that the presence of coastal vegetation would mediate the response of sediment labile organics, microbial community and CO_2 emission to salinity change, such that higher salinity increased CO_2 emission from vegetated habitat but decreased CO_2 emission from non-vegetated habitat (Chen et al., 2022). Consistent with these earlier observations, during the three-year period of our study, the highest annual cumulative CO_2 uptake (brackish marsh) and emission (aquaculture ponds) occurred in 2019, followed by 2020 and 2021 (Figs. 3 and 4), which corresponded to the interannual decline in precipitation recorded by a local weather station: 1807 mm in 2019, 1516 mm in 2020 and 1439 mm in 2021. A higher precipitation would have lowered the *in situ* salinity and led to a higher net CO_2 uptake in a vegetated habitat (e.g., marsh) and higher net CO_2 emission in a non-vegetated habitat (e.g. aquaculture ponds).

In addition to CO_2, organic-rich anoxic sediment also produces CH_4, which is a much stronger greenhouse gas than CO_2 (Bastviken et al., 2008; Li et al., 2020; Rosentreter et al., 2018). In an earlier companion study, the CH_4 fluxes from the brackish marsh and the aquaculture ponds were measured respectively at 1.3 and 17.4 mg CH_4 m^{-2} h^{-1}, for a net increase of 16.1 mg CH_4 m^{-2} h^{-1} emission due to the land conversion (Yang et al. 2022a). Considering that the global warming potential (GWP) of CH_4 is 28 times that of CO_2 on a 100-year time horizon (IPCC, 2014), the total increase in carbon-equivalent emission due to the land use change would be ~948 mg CO_2-eq m^{-2} h^{-1}, with 52% in the form of CO_2 gas (Table 1). While some study has suggested that conversion of coastal marsh to aquaculture ponds affects mainly CH_4 rather than CO_2 (Tan et al., 2020), in the case of the Shanyutan wetland, the effect on CO_2 emission was equally important and should be taken into account when assessing the climate impact of LULCC in this region.

4.4. Recommendations and environmental implications

Several improvements can be considered in future study. Firstly, we only measured anaerobic CO_2 production in the sediment, but aerobic metabolism can occur in the water column, during ebbing tides in the marsh as well as non-culture period in the aquaculture ponds, which should be included in the total CO_2 production (Kauffman et al., 2018; Lovelock et al., 2017; Yang et al., 2018). Due to logistical constraints, gas fluxes were only measured during the daytime, but CO_2 output is expected to increase at night when photosynthesis stops, and our CO_2 fluxes may have been underestimated as a result. Installation of automated gas loggers on site may circumvent this problem. Some shrimp farmers drain the ponds and remove the top sediment during the non-farming period, which would change the carbon dynamics drastically (Kauffman et al., 2018; Sasmito et al., 2019). Comparison of aquaculture ponds with different management practices will shed light on this issue. While newly converted aquaculture ponds are expected to generate high income for the first 5–10 years, productivity often falls off afterward and the ponds are then neglected (Bosma et al., 2012; Cameron et al., 2019); however, these ponds may continue to produce and emit GHGs for a further period of time, and such 'legacy' climate effect also needs to be accounted for. Lastly, our clipped marsh treatment revealed the critical role of vegetation in carbon capture and burial, and therefore reverting unused ponds to vegetated marsh and wetland reforestation could be a sound strategy to offset the climate footprint of the aquaculture sector.

5. Conclusions

This multi-year field study showed that conversion of brackish marsh to aquaculture ponds strongly influenced the system's CO_2 dynamics in the Shanyutan wetland. Land conversion significantly decreased the sediment anaerobic CO_2 production, but increased CO_2 emission notably, turning the system net heterotrophic. Much of the effect may be attributed to the removal of marsh vegetation, with sediment temperature as additional key physical driving factor. The climate impact due to the net increase in CO_2 emission was on-par with the increase in CH_4 emission reported earlier, and therefore should be accounted for when assessing the climate impact of land use change.

Declaration of competing interest

The authors declare that they have no known competing financial interests or personal relationships that could have appeared to influence the work reported in this paper.

Acknowledgements

This research was supported by the Natural Science Foundation of Fujian Province, China (Grant No. 2020J01136, and 2022R1002006), the National Natural Science Foundation of China (Grant No. 41801070, and 41671088), the Research Grants Council of Hong Kong (Grant No. CUHK 14122521, and 14302420) and CUHK Direct Grant (Grant No. 145489489), the Minjiang Scholar Programme.

References

Barroso, G.C., Abril, G., Machado, W., Abuchacra, R.C., Peixoto, R.B., Bernardes, M., Marques, G. S., Sanders, C.J., Oliveira, G.B., Oliveira Filho, S.R., Amora-Nogueira, L., Marotta, H., 2022. Linking eutrophication to carbon dioxide and methane emissions from exposed mangrove soils along an urban gradient. Sci. Total Environ. 850, 157988. https://doi.org/10.1016/j.scitotenv.2022.157988

Bastviken, D., Cole, J.J., Pace, M.L., Van de-Bogert, M.C., 2008. Fates of methane from different lake habitats: Connecting whole-lake budgets and CH_4 emissions. J. Geophys. Res.-Biogeo. 113. 10.1029/2007JG000608

Beaulieu, J.J., DelSontro, T., Downing, J.A., 2019. Eutrophication will increase methane emissions from lakes and impoundments during the 21st century. Nat. Commun. 10, 1375. https://doi.org/10.1038/s41467-019-09100-5

Bhattacharyya, P., Sinhababu, D.P., Roy, K.S., Dash, P.K., Sahu, P.K., Dandapat, R., Neogi, S., Mohanty, S., 2013. Effect of fish species on methane and nitrous oxide emission in relation to soil C, N pools and enzymatic activities in rainfed shallow lowland rice-fish farming system. Agr. Ecosyst. Environ. 176, 53-62. https://doi.org/10.1016/j.agee.2013.05.015

Bosma, R., Sidik, A.S., van Zwieten, P., Aditya, A., Visser, L., 2012. Challenges of a transition to a sustainably managed shrimp culture agro-ecosystem in the Mahakam delta, East Kalimantan, Indonesia. Wetl. Ecol. Manag. 20, 89-99. https://doi.org/10.1007/s11273-011-9244-0

Cameron, C., Hutley, L.B., Friess, D.A., Munksgaard, N.C., 2019. Hydroperiod, soil moisture and bioturbation are critical drivers of greenhouse gas fluxes and vary as a function of landuse change in mangroves of Sulawesi, Indonesia. Sci. Total Environ. 654, 365-377. https://doi.org/10.1016/j.scitotenv.2018.11.092

Chambers, L.G., Osborne, T.Z., Reddy, K.R., 2013. Effect of salinity-altering pulsing events on soil organic carbon loss along an intertidal wetland gradient: a laboratory experiment. Biogeochemistry 115, 363-383. https://doi.org/10.1007/s10533-013-9841-5

Chen, X., Luo, M., Tan, J., Zhang, C.W., Liu, Y.X., Huang, J.F., Xiao, L.L., Xu, Z.H., 2022. Salt-tolerant plant moderates the effect of salinity on soil organic carbon mineralization in a subtropical tidal wetland. Sci. Total Environ. 837, 155855. https://doi.org/10.1016/j.scitotenv.2022.155855

Chmura, G.L., Anisfeld, S.C., Cahoon, D.R., Lynch, J.C., 2003. Global carbon sequestration in tidal, saline wetland soils. Global Biogeochem. Cy. 17, 1111. https://doi.org/10.1029/2002GB001917

Davidson, E.A., Janssens, I.A., 2006. Temperature sensitivity of soil carbon decomposition and feedbacks to climate change. Nature 440, 165-173. https://doi.org/10.1038/nature04514

Duarte, C.M., Losada, I.J., Hendriks, I.E., Mazarrasa, I., Marbà, N., 2013. The role of coastal plant communities for climate change mitigation and adaptation. Nat. Clim. Change 3, 961-968. https://doi.org/10.1038/nclimate1970

Duan, Y.Q., Tian, B., Li, X., Liu, D.Y., Sengupta, D., Wang, Y.J., Peng, Y. 2021. Tracking changes in aquaculture ponds on the China coast using 30 years of Landsat images. Int. J. Appl. Earth Obs. 102, 102383. https://doi. org/10.1016/j.jag.2021.102383

Friedlingstein, P., O'Sullivan, M., Jones, M.W., Andrew, R.M., Hauck, J., Olsen, A., . . . Zaehle, S., 2020. Global Carbon Budget 2020. Earth Syst. Sci. Data 12, 3269-3340. https://doi.org/10.5194/essd-12-3269-2020

Gruca-Rokosz, R., Tomaszek, J.A., Koszelnik, P., Czerwieniec, E. 2011. Methane and carbon dioxide fluxes at the sediment-water interface in reservoirs. Pol. J. Environ. Stud. 20, 81-86

Gruca-Rokosz, R., Tomaszek J.A., 2015. Methane and carbon dioxide in the sediment of a eutrophic reservoir: production pathways and diffusion fluxes at the sediment-water interface. Water Air Soil Poll. 226, 16. https://doi.org/10.1007/s11270-014-2268-3

He, G., Wang, K., Zhong, Q., Zhang, G., van den Bosch, C.K., Wang, J., 2021. Agroforestry reclamations decreased the CO_2 budget of a coastal wetland in the Yangtze estuary. Agri. Forest Meteorol. 296, 108212. https://doi.org/10.1016/j.agrformet.2020.108212

Holgerson, M.A., 2015. Drivers of carbon dioxide and methane supersaturation in small, temporary ponds. Biogeochemistry 124, 305-318. https://doi.org/10.1007/s10533-015-0099-y

Hong, C., Burney, J.A., Pongratz, J., Nabel, J.E.M.S., Mueller, N.D., Jackson, R.B., Davis, S.J., 2021. Global and regional drivers of land-use emissions in 1961–2017. Nature 589, 554-561. https://doi.org/10.1038/s41586-020-03138-ya

Hopkinson, C.S., Cai, W.J., Hu, X., 2012. Carbon sequestration in wetland dominated coastal systems—a global sink of rapidly diminishing magnitude. Curr. Opin. Env. Sust. 4, 186-194. https://doi.org/10.1016/j.cosust.2012.03.005

Hsieh, S.-H., Yuan, C.-S., Ie, I.-R., Yang, L., Lin, H.-J., Hsueh, M.-L., 2021. In-situ measurement of greenhouse gas emissions from a coastal estuarine wetland using a novel continuous monitoring technology: Comparison of indigenous and exotic plant species. J. Environ. Manage. 281, 111905. https://doi.org/10.1016/j.jenvman.2020.111905

IPCC, 2014. Climate change 2014: Synthesis report. Contribution of working groups I, II and III to the fifth assessment report of the Intergovernmental Panel on Climate Change. Geneva, Switzerland: IPCC.

Kauffman, J., Bernardino, A., Ferreira, T., Bolton, N., Gomes, L. E., Nóbrega, G., 2018. Shrimp ponds lead to massive loss of soil carbon and greenhouse gas emissions in northeastern Brazilian mangroves. Ecol. Evol. 8. https://doi.org/10.1002/ece3.4079

Kelker, D., Chanton, J., 1997. The effect of clipping on methane emission from *Cares*. Biogeochemistry 39, 37-44. https://doi.org/10.1002/ece3.4079

Kirwan, M.L., Mudd, S.M., 2012. Response of salt-marsh carbon accumulation to climate change. Nature 489, 550-553. https://doi.org/10.1038/nature 11440

Le Quéré, C., Andrew, R. M., Friedlingstein, P., Sitch, S., Hauck, J., Pongratz, J., . . . Zheng, B., 2018. Global Carbon Budget 2018. Earth Syst. Sci. Data 10, 2141-2194. https://doi.org/10.5194/essd-10-2141-2018

Li, X.F., Lai, D.Y.F., Gao, D.Z., 2020. Anaerobic oxidation of methane with denitrification in sediments of a subtropical estuary: Rates, controlling factors and environmental implications. J. Environ. Manage. 273, 111151. https://doi.org/10.1016/j.jenvman.2020.111151

Li, Y.L., Ge, Z.M., Xie, L.N., Li, S.H., Tan, L.S., Hancke, K., 2022. Effects of waterlogging and elevated salinity on the allocation of photosynthetic carbon in estuarine tidal marsh: a mesocosm experiment. Plant Soil 482, 211-227. https://doi.org/10.1007/s11104-022-05687-9

Liu, J.G., Hartmann, S C., Keppler, F., Lai, D.Y.F., 2019. Simultaneous abiotic production of greenhouse gases (CO_2, CH_4, and N_2O) in Subtropical Soils. J. Geophys. Res.-Biogeo. 124, 1977-1987. https://doi.org/10.1029/2019JG005154

Lovelock, C.E., Fourqurean, J.W., Morris, J.T., 2017. Modeled CO_2 emissions from coastal wetland transitions to other land uses: tidal marshes, mangrove forests, and seagrass beds. Front. Mar. Sci. 4, 143. https://doi.org/10.3389/fmars.2017.00143

Luo, J.H., Sun, Z., Lu, L.R., Xiong, Z.Y., Cui, L.P., Mao, Z.G., 2022. Rapid expansion of coastal aquaculture ponds in Southeast Asia: Patterns, drivers and impacts. J. Environ. Manage. 315, 115100. https://doi.org/10.1016/j.jenvman.2022.115100

Magenheimer, J.F., Moore, T.R., Chmura, G.L., Daoust, R.J., 1996. Methane and carbon dioxide flux from a macrotidal salt marsh, Bay of Fundy, New Brunswick. Estuaries 19, 139-145. https://doi.org/10.2307/1352658

Matos, C.R.L., Mendoza, U., Diaz, R., Moreira, M., Belem, A.L., Metzger, E., Albuquerque, A.L.S., Machado, W., 2016. Nutrient regeneration susceptibility under contrasting sedimentary conditions from the Rio de Janeiro coast, Brazil. Mar. Pollut. Bull. 108, 297-302. https://doi.org/10.1016/j.marpolbul.2016.04.046

Mcleod, E., Chmura, G.L., Bouillon, S., Salm, R., Björk, M., Duarte, C.M., Lovelock, C.E., Schlesinger, W.H., Silliman, B.R., 2011. A blueprint for blue carbon: toward an improved understanding of the role of vegetated coastal habitats in sequestering CO_2. Front. Ecol. Environ. 9, 552-560. https://doi.org/10.1890/110004

Meng, W., Hu, B., He, M., Liu, B., Mo, X., Li, H., Wang, Z., Zhang, Y., 2017. Temporal-spatial variations and driving factors analysis of coastal reclamation in China. Estuar. Coast. Shelf S. 191, 39-49. https://doi.org/10.1016/j.ecss.2017.04.008

Meng, W., Feagin, R. A., Hu, B., He, M., Li, H., 2019. The spatial distribution of blue carbon in the coastal wetlands of China. Estuar. Coast. Shelf S. 222, 13-20.

Mitsch, W.J., Bernal, B., Nahlik, A.M., Mander, Ü., Zhang, L.I., Anderson, C.J., Jørgensen, S.E., Brix, H., 2013. Wetlands, carbon, and climate change. Landscape Ecol. 28, 583-597. https://doi.org/10.1007/s10980-012-9758-8

Murray, N.J., Phinn, S.R., DeWitt, M., Ferrari, R., Johnston, R., Lyons, M.B., Clinton, N., Thau, D., Fuller, R.A., 2019. The global distribution and trajectory of tidal flats. Nature 565, 222-225. https://doi.org/10.1038/s41586-018-0805-8

Naskar, S., Pailan, G.H., Datta, S., Sawant, P.B., Bharti, V.S., 2020. Effect of different organic manures and salinity levels on greenhouse gas emission and growth of common carp in aquaculture systems. Aquac. Res. 52, 1-10. https://doi.org/10.1111/are.15041

Natchimuthu, S., Sundgren, I., Gålfalk, M., Klemedtsson, L., Bastviken, D., 2017. Spatiotemporal variability of lake $p\mathrm{CO_2}$ and CO_2 fluxes in a hemiboreal catchment. J. Geophys. Res.-Biogeo. 122, 30-49. https://doi.org/10.1002/2016JG003449

Neubauer, S., Franklin, R., Berrier, D., 2013. Saltwater intrusion into tidal freshwater marshes alters the biogeochemical processing of organic carbon. Biogeosciences 10, 8171-8183. https://doi.org/10.5194/bg-10-8171-2013

Ottinger, M., Clauss, K., Kuenzer, C., 2016. Aquaculture: Relevance, distribution, impacts and spatial assessments – A review. Ocean Coast. Manage. 119, 244-266. https://doi.org/10.1016/j.ocecoaman.2015.10.015

Pendleton, L., Donato, D.C., Murray, B.C., Crooks, S., Jenkins, W.A., Sifleet, S., Craft, C., Fourqurean, J.W., Kauffman, J.B., Marbà, N., Megonigal, P., Pidgeon, E., Herr, D., Gordon, D., Baldera, A., 2012. Estimating global “blue carbon” emissions from conversion and degradation of vegetated coastal ecosystems. PLOS ONE 7, e43542. https://doi.org/10.1371/journal.pone.0043542

Ren, C.Y., Wang, Z.M., Zhang, Y.Z., Zhang, B., Chen, L., Xia, Y.B., Xiao, X.M., Doughty, R.B., Liu, M.Y., Jia, M., Mao, D.H., Song, K.S., 2019. Rapid expansion of coastal aquaculture ponds in China from Landsat observations during 1984–2016. Int. J. Appl. Earth Obs. 82, 101902. https://doi.org/10.1016/j.jag.2019.101902

Rosentreter, J.A., Maher, D.T., Erler, D.V., Murray, R.H., Eyre, B.D., 2018. Methane emissions partially offset “blue carbon” burial in mangroves. Sci. Adv. 4, eaao4985. https://doi.org/10.1126/sciadv.aao4985

Sasmito, S.D., Taillardat, P., Clendenning, J.N., Cameron, C., Friess, D.A., Murdiyarso, D., Hutley, L.B., 2019. Effect of land-use and land-cover change on mangrove blue carbon: A systematic review. Global Change Biology 25, 4291-4302. https://doi.org/10.1111/gcb.14774

Sepulveda-Jauregui, A., Hoyos-Santillan, J., Martinez-Cruz, K., Anthony, K.M.W., Casper, P., Belmonte-Izquierdo, Y., Thalasso, F., 2018. Eutrophication exacerbates the impact of climate warming on lake methane emission. Sci. Total Environ. 636, 411-419. https://doi.org/10.1016/j.scitotenv.2018.04.283

Šímová, I., Sandel, B., Enquist, B.J., Michaletz, S.T., Kattge, J., Violle, C., McGill, B.J., Blonder, B., Engemann, K., Peet, R.K., Wiser, S.K., Morueta-Holme, N., Boyle, B., Kraft, N.J.B., Svenning, J.C., 2019. The relationship of woody plant size and leaf nutrient content to large-scale productivity for forests across the Americas. J. Ecol. 107, 2278-2290. https://doi.org/10.1111/1365-2745.13163

Suweis, S., Carr, J.A., Maritan, A., Rinaldo, A., D’Odorico, P., 2015. Resilience and reactivity of global food security. PNAS 112, 6902-6907. doi:10.1073/pnas.1507366112

Tan, L.S., Ge, Z.M., Zhou, X.H., Li, S.H., Li, X.Z., Tang, J.W., 2020. Conversion of coastal wetlands, riparian wetlands, and peatlands increases greenhouse gas emissions: A global meta-analysis. Global Change Biol. 26, 1638-1653. https://doi.org/10.1111/gcb.14933

Tan, L.S., Ge, Z.M., Ji, Y.H., Lai, D.Y.F., Temmerman, S., Li, S.H., Li, X.Z., Tang, J.W., 2022. Land use and land cover changes in coastal and inland wetlands cause soil carbon and nitrogen loss. Global Ecol. Biogeogr. 31, 2541-2563. https://doi.org/10.1111/geb.13597

Tong, C., Wang, W.Q., Zeng, C.S., Marrs, R., 2010. Methane (CH_4) emission from a tidal marsh in the Min River estuary, southeast China. J. Environ. Sci. Heal. A 45, 506-516. https://doi.org/10.1080/10934520903542261

Tong, C., Wang, W.Q., Huang, J.F., Gauci, V., Zhang, L.H., Zeng, C.S., 2012. Invasive alien plants increase CH_4 emissions from a subtropical tidal estuarine wetland. Biogeochemistry 111, 677-693. https://doi.org/10.1007/s10533-012-9712-5

Tong, C., Morris, J.T., Huang, J.F., Xu, H., Wan, S.A., 2018. Changes in pore-water chemistry and methane emission following the invasion of *Spartina alterniflora* into an oliogohaline marsh. Limnol. Oceanog. 63, 384-396. https://doi.org/10.1002/lno.10637

Wang, W.Q., Sardans, J., Wang, C., Zeng, C.S., Tong, C., Asensio, D., Peñuelas, J., 2017. Relationships between the potential production of the greenhouse gases CO_2, CH_4 and N_2O and soil concentrations of C, N and P across 26 paddy fields in southeastern China. Atmos. Environ. 164, 458-467. http://dx.doi.org/10.1016/j.atmosenv.2017.06.023

Wang, M., Mao, D., Xiao, X., Song, K., Jia, M., Ren, C., Wang, Z., 2023. Interannual changes of coastal aquaculture ponds in China at 10-m spatial resolution during 2016–2021. Remote Sens. Environ. 284, 113347. https://doi.org/10.1016/j.rse.2022.113347

World Meteorological Organization, 2022. WMO provisional state of the global climate 2022.

Xing, Y.P., Xie, P., Yang, H., Ni, L. Y., Wang, Y.S., Rong, K.W., 2005. Methane and carbon dioxide fluxes from a shallow hypereutrophic subtropical Lake in China. Atmos. Environ. 39, 5532-5540. https://doi.org/10.1016/j.atmosenv.2005.06.010

Xu, C., Su, G., Zhao, K., Xu, X., Li, Z., Hu, Q., Xue, Y., Xu, J. 2022. Current status of greenhouse gas emissions from aquaculture in China. Water Biol. Secur. 1, 100041. https://doi.org/10.1016/j.watbs.2022.100041

Yang, P., Lai, D.Y.F., Huang, J.F., Tong, C., 2018. Effect of drainage on CO_2, CH_4, and N_2O fluxes from aquaculture ponds during winter in a subtropical estuary of China. J. Environ. Sci. 65, 72-82. https://doi.org/10.1016/j.jes.2017.03.024

Yang, P., Lai, D.Y.F., Yang, H., Lin, Y., Tong, C., Hong, Y., Tian, Y. L., Tang, C., Tang, K. W. 2022a. Large increase in CH_4 emission following conversion of coastal marsh to aquaculture ponds caused by changing gas transport pathways. Water Res. 222, 118882. https://doi.org/10.1016/j.watres.2022.118882

Yang, P., Tang, K.W., Tong, C., Lai, D.Y.F., Zhang, L.H., Lin, X., Yang, H., Tan, L.S., Zhang, Y.F., Hong, Y., Tang, C., Lin, Y.X. 2022b. Conversion of coastal wetland to aquaculture ponds decreased N_2O emission: Evidence from a multi-year field study. Water Res. 227, 119326. https://doi.org/10.1016/j.watres.2022.119326

Yang, P., Tang, K.W., Tong, C., Lai, D.Y.F., Wu, L., Yang, H., Zhang, L., Tang, C., Hong, Y., Zhao, G., 2022c. Changes in sediment methanogenic archaea community structure and methane production potential following conversion of coastal marsh to aquaculture ponds. Environ. Pollut. 305, 119276. https://doi.org/10.1016/j.envpol.2022.119276

Yang, P., Zhang, L.H., Lai, D.Y.F., Yang, H., Tan, L.S., Luo, L.J., Tong, C., Hong, Y., Zhu, W.Y., Tang, K.W., 2022d. Landscape change affects soil organic carbon mineralization and greenhouse gas production in coastal wetlands. Global Biogeochem. Cy. 36, e2022GB007469. https://doi.org/10.1029/2022GB007469

Yao, L., Adame, M.F., Chen, C., 2021. Resource stoichiometry, vegetation type and enzymatic activity control wetlands soil organic carbon in the Herbert River catchment, North-east Queensland. J. Environ. Manage. 296, 113183. https://doi.org/10.1016/j.jenvman.2021.113183

Ye, W.W., Sun, H., Li, Y.H, Zhang, J.X., Zhang, M.M., Gao, Z.Y., Yan, J.P., Liu, J., Wen, J.W., Yang, H., Shi, J., Zhao, S.H., Wu, M., Xu, S.Q., Xu, C.A., Zhan, L.Y., 2022. Greenhouse gas emissions from fed mollusk mariculture: a case study of a *Sinonovacula constricta* farming system. Agr. Ecosyst. Environ. 336, 108029. https://doi.org/10.1016/j.agee.2022.108029

Yuan, J., Ding, W., Liu, D., Kang, H., Freeman, C., Xiang, J., Lin, Y., 2015. Exotic Spartina alterniflora invasion alters ecosystem–atmosphere exchange of CH_4 and N_2O and carbon sequestration in a coastal salt marsh in China. Global Change Biol. 21, 1567-1580. https://doi.org/10.1111/gcb.12797

Yuan, J., Xiang, J., Liu, D., Kang, H., He, T., Kim, S., Lin, Y., Freeman, C., Ding, W., 2019. Rapid growth in greenhouse gas emissions from the adoption of industrial-scale aquaculture. Nat. Clim. Change 9, 318-322. https://doi.org/10.1038/s41558-019-0425-9

Zhang, Y., Yang, P., Yang, H., Tan, L., Guo, Q., Zhao, G., Li, L., Gao, Y., Tong, C., 2019. Plot-scale spatiotemporal variations of CO_2 concentration and flux across water-air interfaces at aquaculture shrimp ponds in a subtropical estuary. Environ. Sci. Pollut. R. 26, 5623-5637. https://doi.org/10.1007/s11356-018-3929-3

Zhang, Y., Tang, K. W., Yang, P., Yang, H., Tong, C., Song, C., Tan, L., Zhao, G., Zhou, X., Sun, D., 2022. Assessing carbon greenhouse gas emissions from aquaculture in China based on aquaculture system types, species, environmental conditions and management practices. Agr. Ecosyst. Environt 338, 108110. https://doi.org/10.1016/j.agee.2022.108110

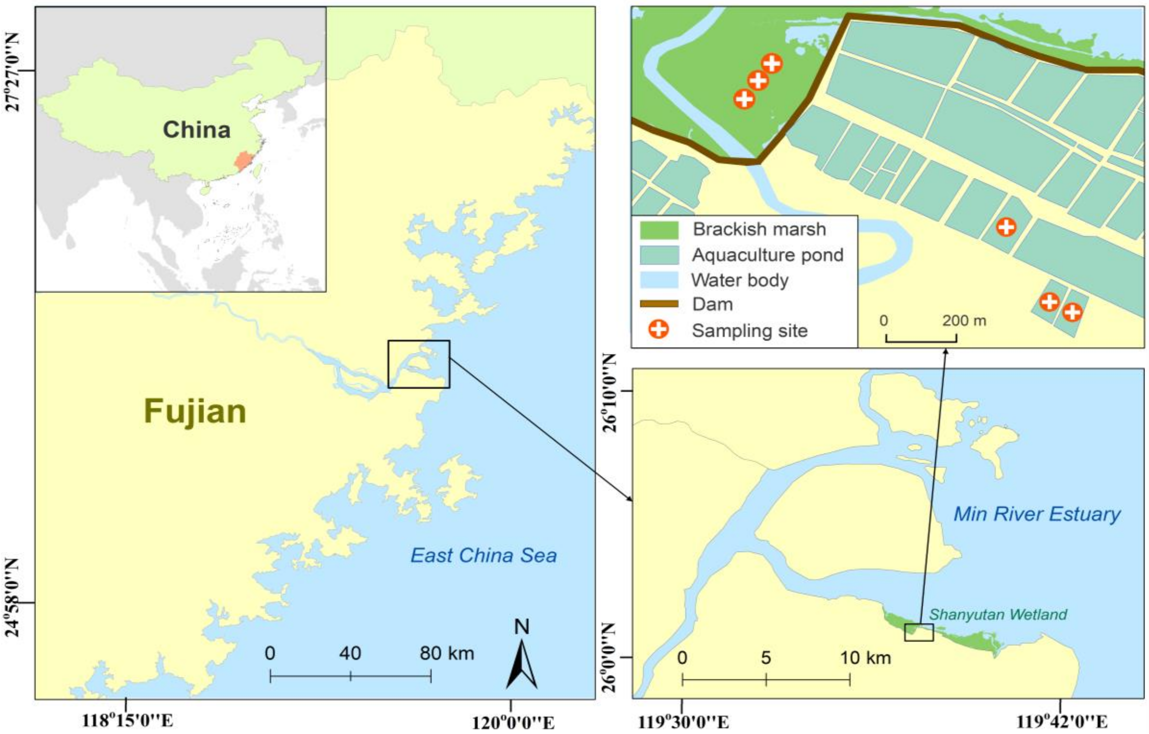

Figure 1. The location of the sampling sites in the brackish marsh and aquaculture ponds in Shanyutan Wetland within the Min River Estuary.

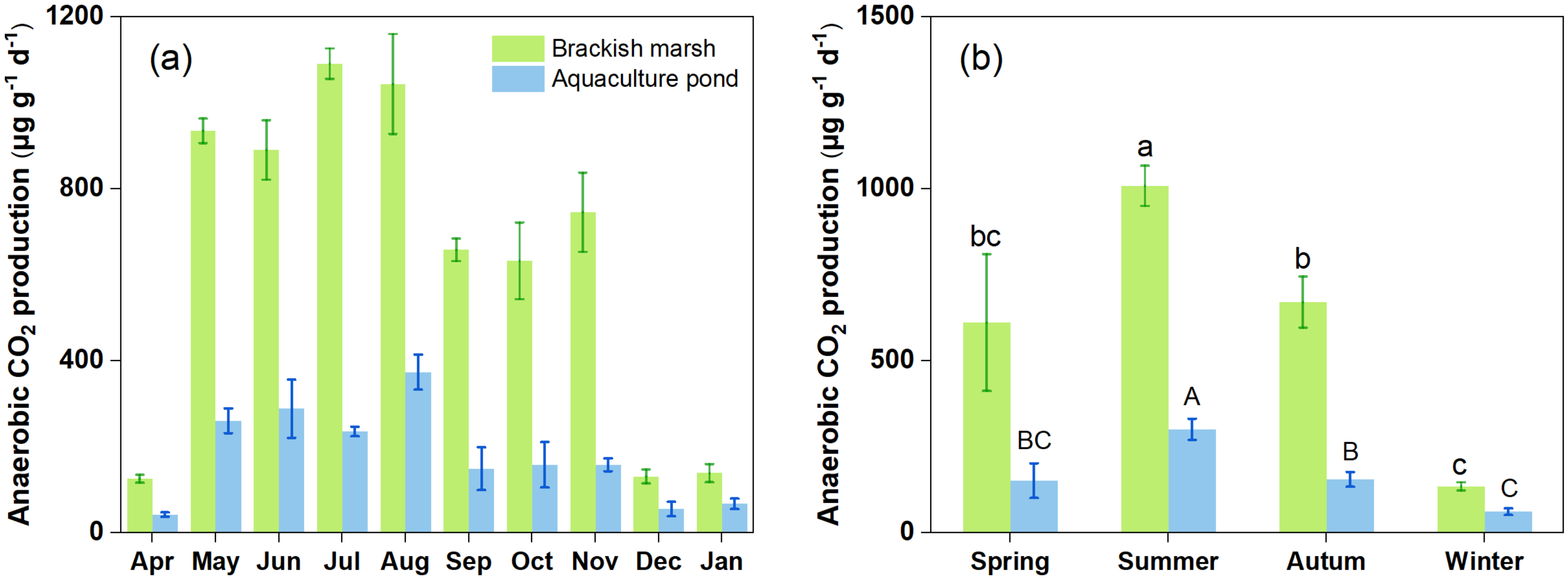

Figure 2. Monthly (a) and seasonal (b) variations of sediment CO_2 production potential (mean ± S.E.) between brackish marsh and aquaculture ponds. Different lowercase and uppercase letters indicate significant differences of sediment CO_2 production potential across four seasons in brackish marsh and aquaculture ponds, respectively.

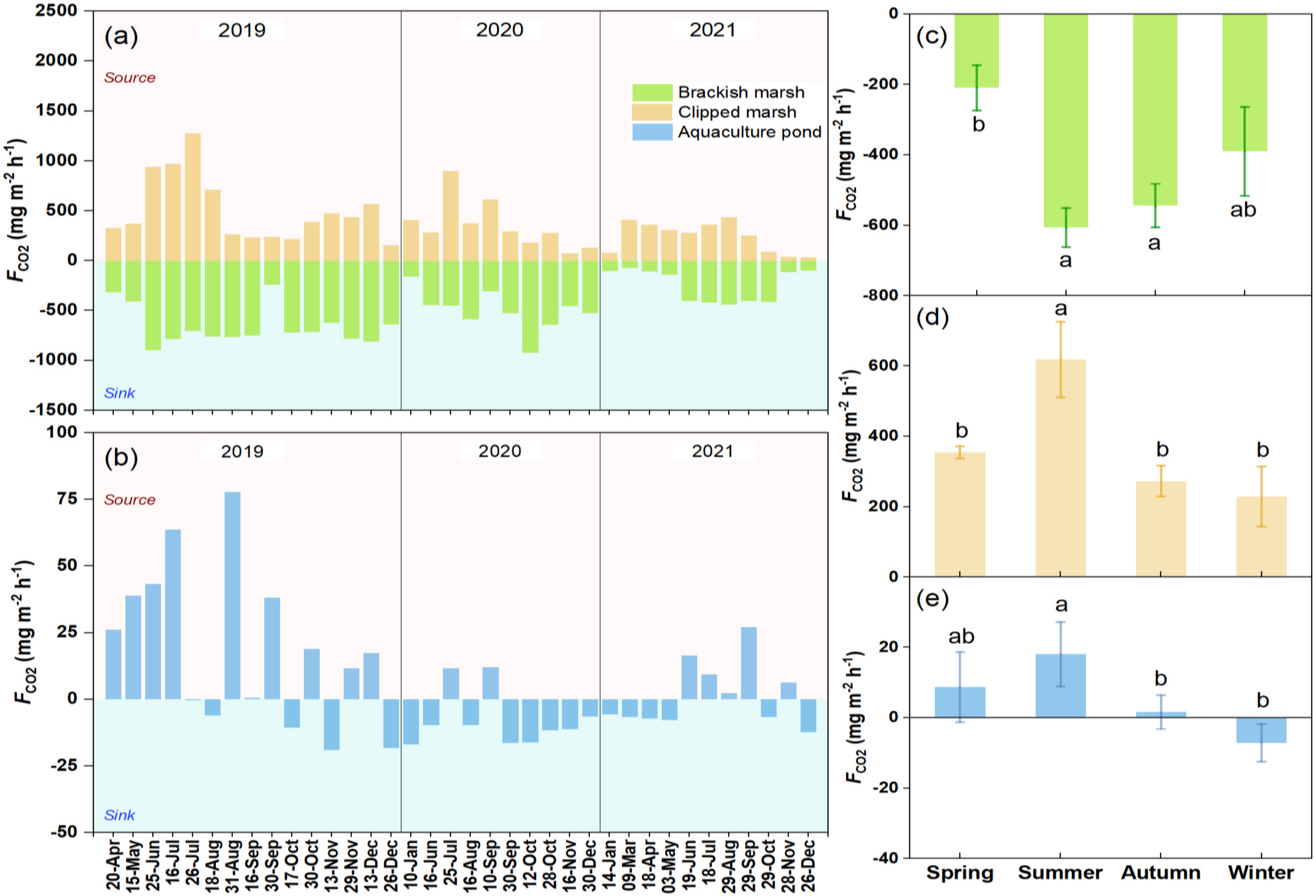

Figure 3. Monthly (a, b) and seasonal (c, d, e) variations of CO_2 flux (mean ± S.E.) among brackish marsh, clipped marsh and aquaculture ponds. Different letters indicate significant differences of sediment CO_2 production potential across four seasons.

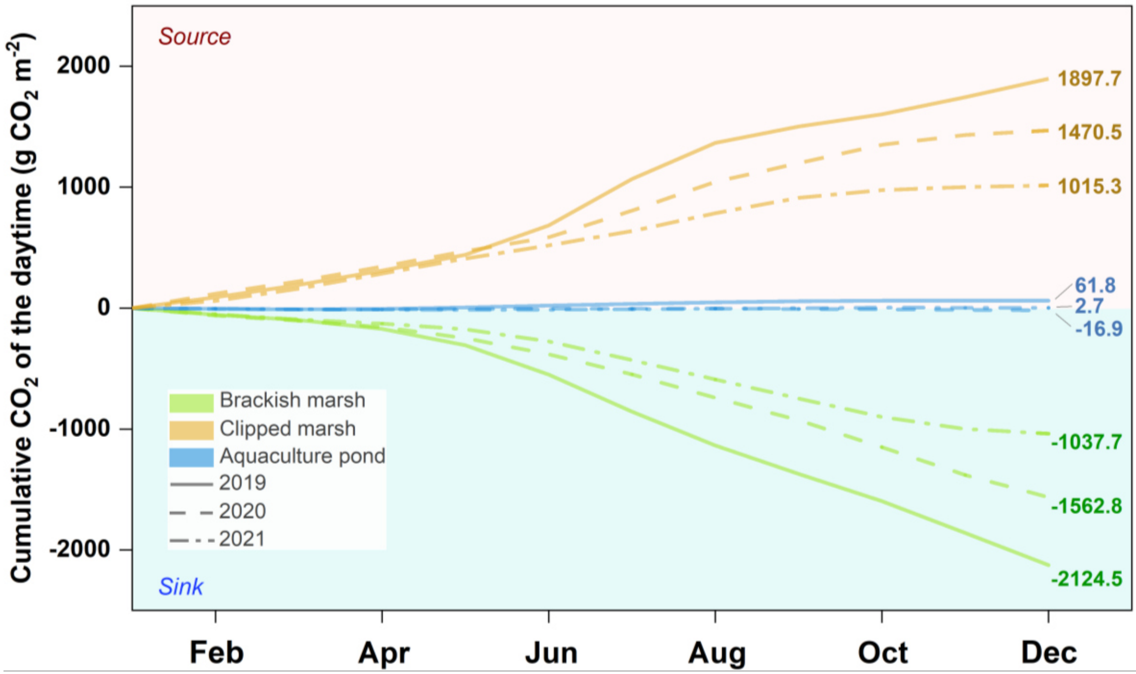

Figure 4. Cumulative CO_2 fluxes among brackish marsh, clipped marsh and aquaculture ponds during the measurement period.

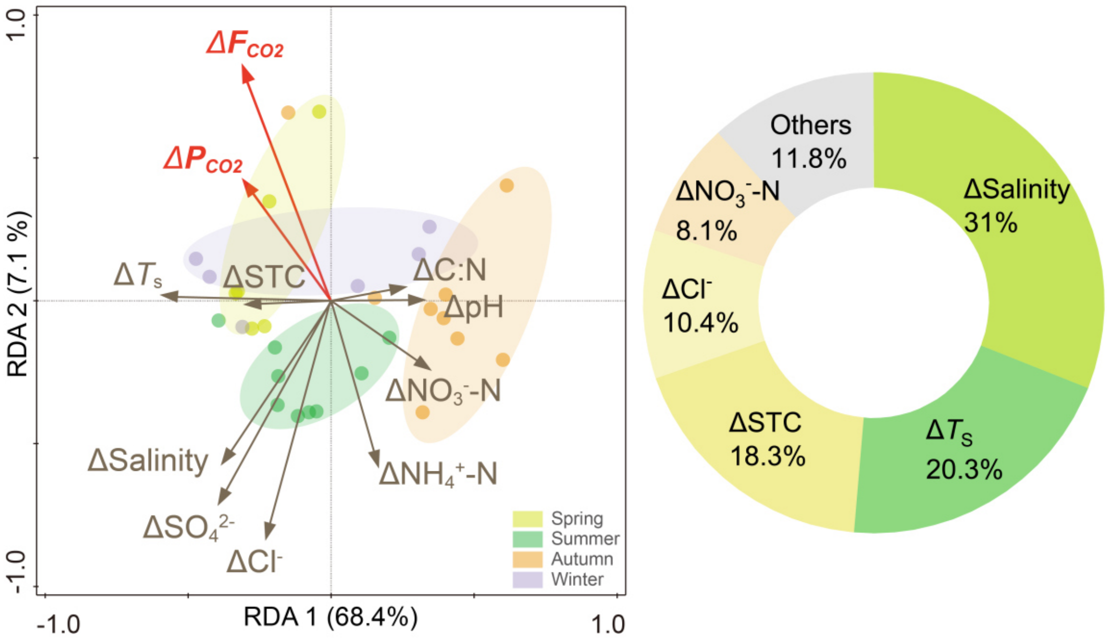

Figure 5. Redundancy analysis (RDA) of the relationship between the change rate of CO_2 production potential (ΔP_{CO2}) as well as fluxes (ΔF_{CO2}) and the change rate of environmental factors after land conversion. The pie charts show the percentages of relative influence of environmental factors on ΔF_{CO2} and ΔP_{CO2}.

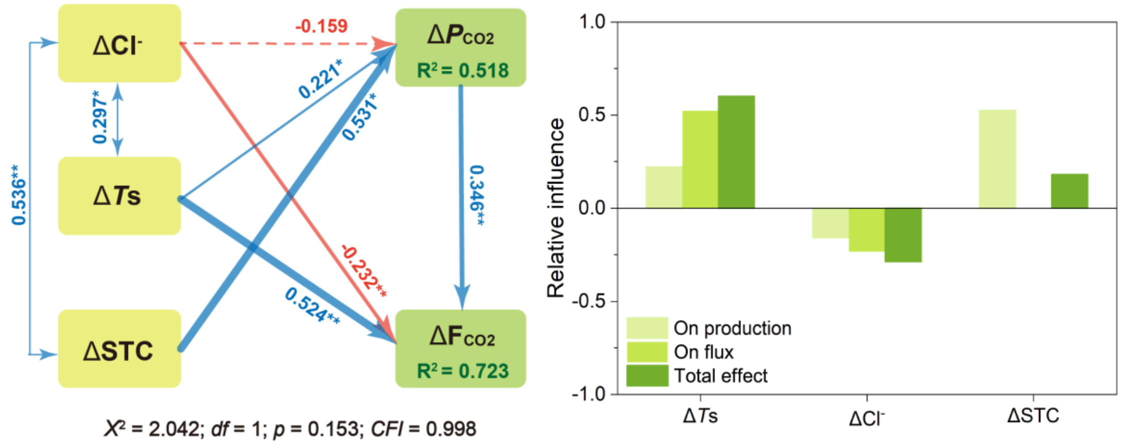

Figure 6. Partial least square structural equation modeling (PLS-SEM) of the change rate of CO_2 production potential (ΔP_{CO2}) and fluxes (ΔF_{CO2}) response to the change rate of environmental factors caused by land conversion. Boxes indicate measured variables used in the model. The solid blue and red arrows indicate significant positive and negative effects, respectively, and the dotted arrow indicates insignificant effect on the dependent variable. Numbers adjacent to arrows are standardized path coefficients, indicating the effect size of the relationship. R^2 represents the variance explained for target variables. * $p < 0.05$; ** $p < 0.01$.

Table 1

The global warming potential and carbon emission of brackish marsh, clipped marsh and aquaculture ponds.

Habitat type	**CO_2 flux (mg CO_2 m^{-2} h^{-1})**	**CH_4 flux* (mg CH_4 m^{-2} h^{-1})**	**C emission (mg C m^{-2} h^{-1})**	**GWP (mg CO_2-eq m^{-2} h^{-1})**
Brackish marsh	-490.8	1.3	-11.1	-453.3
Clipped marsh	382.6	0.3	8.7	391.3
Aquaculture ponds	6.2	17.4	1.2	493.4

*Data was from Yang et al. (2022a). Global warming potential (GWP, mg CO_2-eq m^{-2} h^{-1}) from CO_2 and CH_4 fluxes was calculated. The radiative forcing constant of CH_4 is 28 times relative to CO_2 equivalent at the 100-year time horizon (IPCC 2014).

Supporting Information

Effects of conversion of coastal marshes to aquaculture ponds on sediment anaerobic CO_2 production and emission in a subtropical estuary of China

Lishan Tan[a,b], Linhai Zhang[a,b], Ping Yang[a,b,c,d*], Chuan Tong[a,b,d], Derrick Y.F. Lai[e], Hong Yang[f,g], Yan Hong[a], Yalan Tian[a], Chen Tang[a], Manjing Ruan[a], Kam W. Tang[h*]

[a]*School of Geographical Sciences, Fujian Normal University, Fuzhou 350117, P.R. China*

[b]*Institute of Geography, Fujian Normal University, Fuzhou 350117, P.R. China*

[c]*Fujian Provincial Key Laboratory for Subtropical Resources and Environment, Fujian Normal University, Fuzhou 350117, P.R. China*

[d]*Key Laboratory of Humid Subtropical Eco-geographical Process of Ministry of Education, Fujian Normal University, Fuzhou 350117, P.R. China*

[e]*Department of Geography and Resource Management, The Chinese University of Hong Kong, Hong Kong, China*

[f]*College of Environmental Science and Engineering, Fujian Normal University, Fuzhou 350007, P.R. China*

[g]*Department of Geography and Environmental Science, University of Reading, Reading, RG6 6AB, UK*

[h]*Department of Biosciences, Swansea University, Swansea SA2 8PP, U. K.*

***Correspondence to:**

Ping Yang (yangping528@sina.cn); Kam W. Tang (k.w.tang@swansea.ac.uk)

Telephone: 086-0591-87445659 **Fax:** 086-0591-83465397

Supporting Information Summary

No. of pages: 7   No. of method description: 1   No. of figures: 3

No. of tables: 0

Page S3: Measurement of CO_2 concentration.

Page S4: Figure S1. Boxplots of (a) sediment temperature (T_S); (b) sediment salinity; (c) sediment pH; (d) sediment total carbon (STC) content; (e) sediment total nitrogen (STN) content; (f) porewater SO_4^{2-} concentration; (g) porewater Cl^- concentration; (h) porewater NO_3^--N concentration; (i) porewater NH_4^+-N concentration in brackish marsh and aquaculture ponds. * and ** indicate significant differences between summer and winter at levels of $p < 0.05$ and $p < 0.01$, respectively. Data are after *Yang et al.* [2022a, 2022b] for reference and review only.

Page S5: Figure S2. Redundancy analysis (RDA) of the relationship between CO_2 fluxes (F_{CO2}) (and CO_2 production potential, P_{CO2}) and environmental factors between brackish marsh (a) and aquaculture ponds (b). The pie charts show the percentages of relative influence of environmental factors on F_{CO2} and P_{CO2}.

Page S6: Figure S3. Partial least square structural equation modeling (PLS-SEM) of the effect of environmental factors on CO_2 fluxes and CO_2 production potential among brackish marsh (a) and aquaculture ponds (b). Boxes indicate measured variables entered in the model. The solid blue and red arrows indicate significant positive and negative effects, respectively, and the dotted arrows indicate insignificant effects on dependent variables. Numbers adjacent to arrows are standardized path coefficients, indicating the effect size of the relationship. R^2 represents the variance explained for target variables. * $p < 0.05$; ** $p < 0.01$.

Method description

Measurement of CO_2 concentration

CO_2 concentrations were measured using a gas chromatograph (GC-2014, Shimadzu, Japan) equipped with a flame ionization detector (FID); The column and detector temperatures were set at 45°C and 280 °C, respectively; The flow rate of nitrogen (the carrier gas) was set at 30 mL min^{-1}, while the flow rate of air and H_2 for the FID were set at 400- and 40-mL min^{-1}, respectively. The gas chromatograph system was Nanjing Special Gas Co., Ltd (low standard CO_2 = 395 ppm; high standard CO_2 = 3090 ppm). The mean analytical precision of individual measurements was 5%.

The CO_2 emission flux was calculated using a linear regression of the changes in the gas concentrations inside the chamber and the measured time, base area, chamber volume, and the molar volume of CO_2 at ambient temperature (Hirota et al., 2004; Helton et al., 2014). Similarly, a linear regression was also used for calculation of CO_2 production rate (Liu et al., 2019; Wang et al., 2017).

The minimum detectable concentration difference of CO_2 was ±1.0 ppmv, which was calculated uses replicates of standards. All CO_2 emission fluxes and production rates were above the minimum detectable concentration difference. We excluded the fluxes and production rates with poor linear relationships (i.e., $r^2 < 0.90$) from further analysis. The majority of flux measurements had regression coefficients of $r^2 > 0.90$.

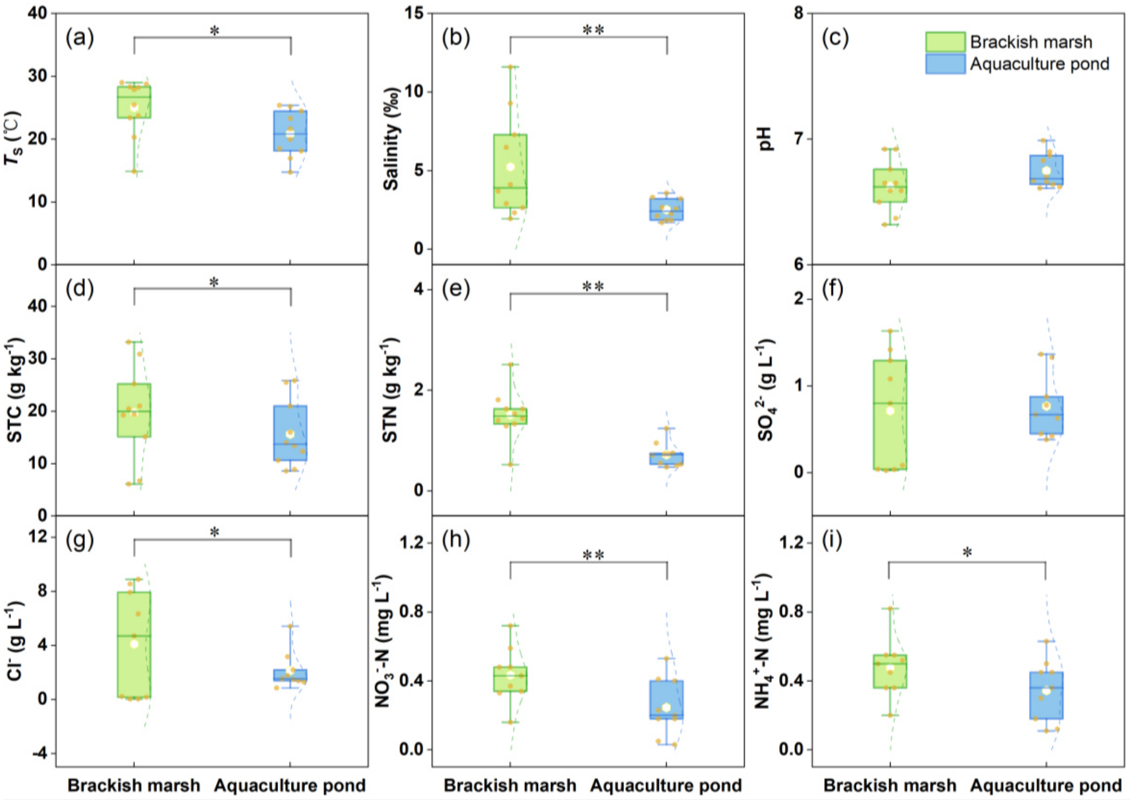

Figure S1. Boxplots of (a) sediment temperature (T_S); (b) sediment salinity; (c) sediment pH; (d) sediment total carbon (STC) content; (e) sediment total nitrogen (STN) content; (f) porewater SO_4^{2-} concentration; (g) porewater Cl^- concentration; (h) porewater NO_3^--N concentration; (i) porewater NH_4^+-N concentration in brackish marsh and aquaculture ponds. * and ** indicate significant differences between summer and winter at levels of $p < 0.05$ and $p < 0.01$, respectively. Data are after *Yang et al.* [2022a, 2022b] for reference and review only.

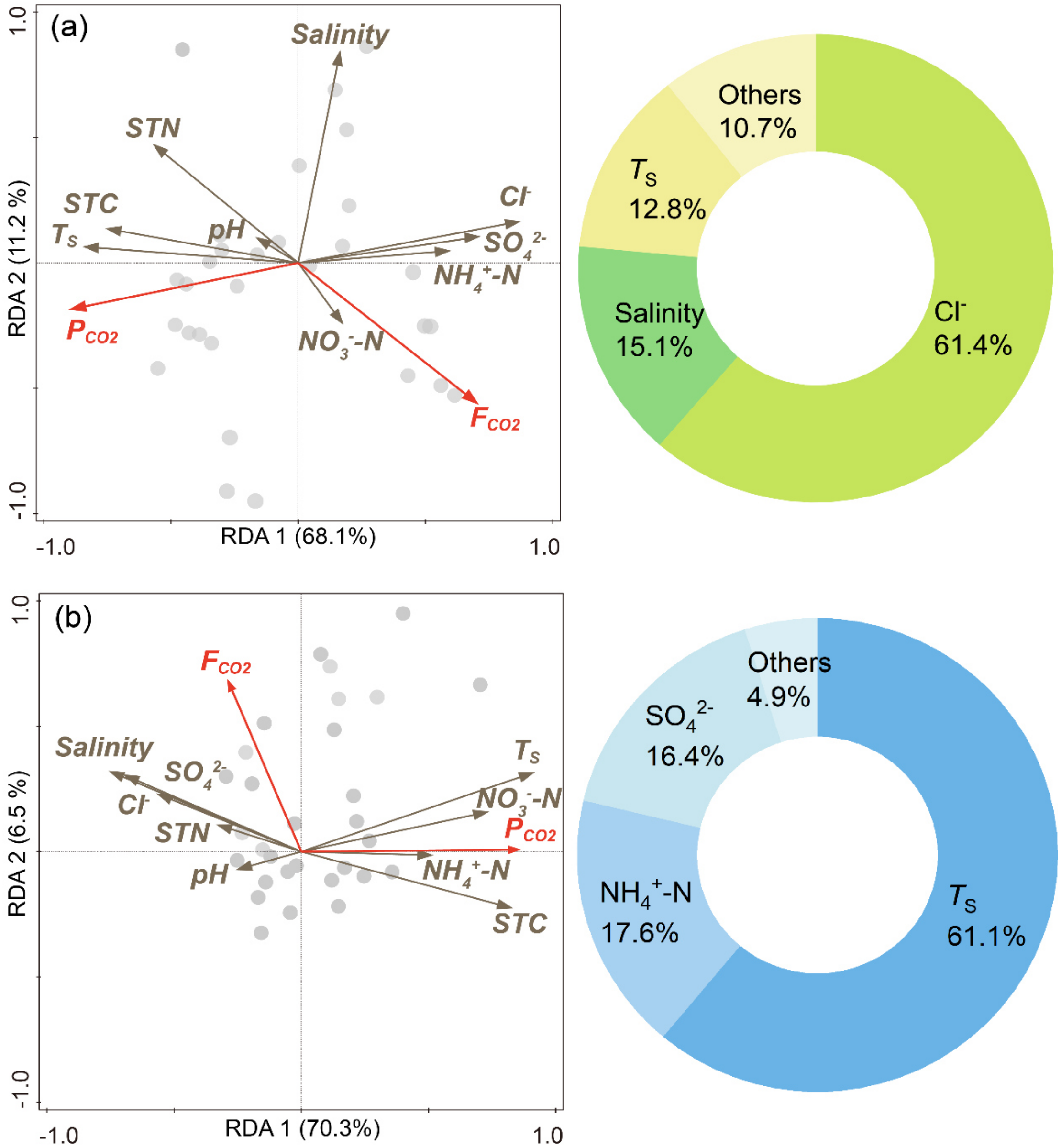

Figure S2. Redundancy analysis (RDA) of the relationship between CO_2 fluxes (F_{CO2}) (and CO_2 production potential, P_{CO2}) and environmental factors between brackish marsh (a) and aquaculture ponds (b). The pie charts show the percentages of relative influence of environmental factors on F_{CO2} and P_{CO2}.

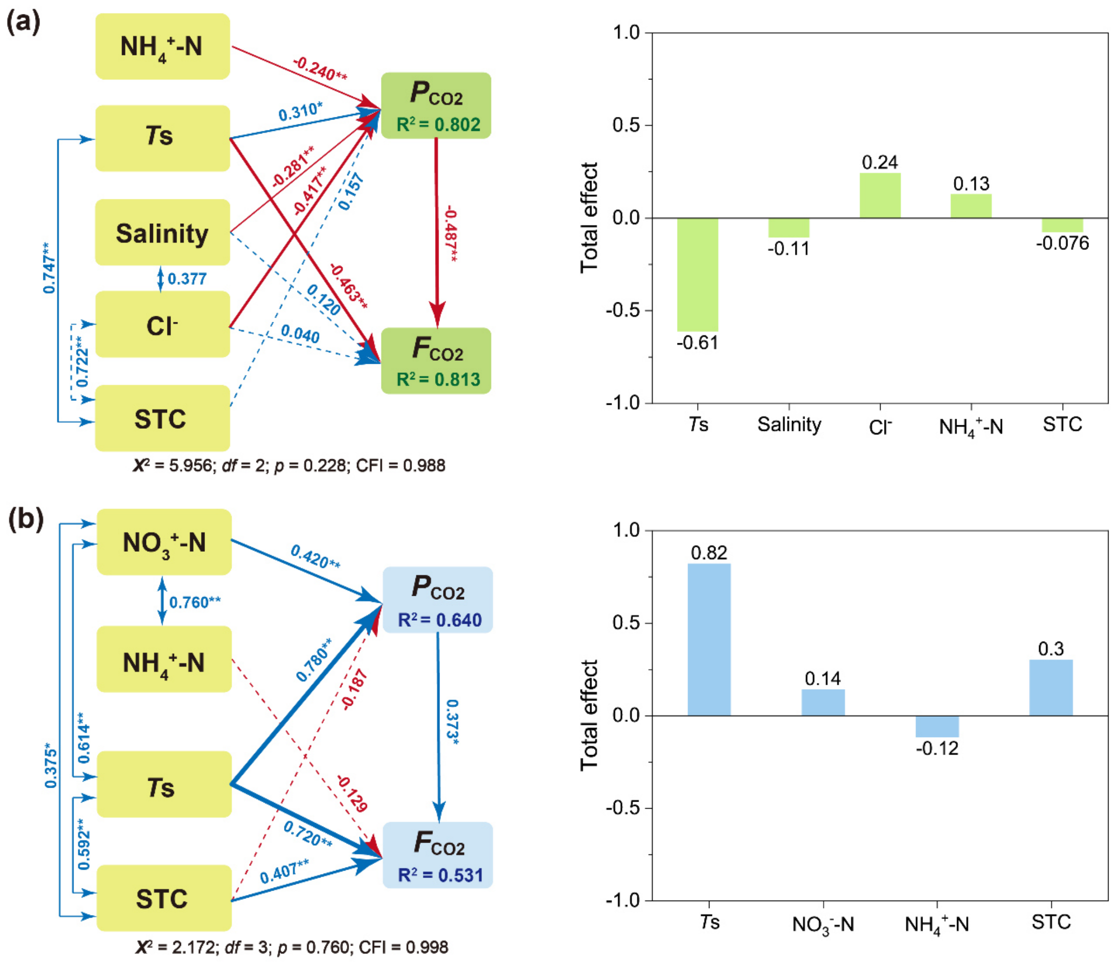

Figure S3. Partial least square structural equation modeling (PLS-SEM) of the effect of environmental factors on CO_2 fluxes and CO_2 production potential among brackish marsh (a) and aquaculture ponds (b). Boxes indicate measured variables entered in the model. The solid blue and red arrows indicate significant positive and negative effects, respectively, and the dotted arrows indicate insignificant effects on dependent variables. Numbers adjacent to arrows are standardized path coefficients, indicating the effect size of the relationship. R^2 represents the variance explained for target variables. * $p < 0.05$; ** $p < 0.01$.

Reference

Hirota, M., Tang, Y., Hu, Q., Hirata, S., Kato, T., Mo, W., Cao, G., Mariko, S., 2004. Methane emissions from different vegetation zones in a Qinghai-Tibetan Plateau wetland. Soil Biology and Biochemistry 36, 737-748. https://doi.org/10.1016/j.soilbio.2003.12.009

Helton, A.M., Bernhardt, E.S., Fedders, A., 2014. Biogeochemical regime shifts in coastal landscapes: the contrasting effects of saltwater incursion and agricultural pollution on greenhouse gas emissions from a freshwater wetland. Biogeochemistry 120, 133-147. https://doi.org/10.1007/s10533-014-9986-x

Liu, J.G., Hartmann, S C., Keppler, F., Lai, D.Y.F., 2019. Simultaneous abiotic production of greenhouse gases (CO_2, CH_4, and N_2O) in Subtropical Soils. J. Geophys. Res.-Biogeo. 124, 1977-1987. https://doi.org/10.1029/2019JG005154

Wang, W.Q., Sardans, J., Wang, C., Zeng, C.S., Tong, C., Asensio, D., Peñuelas, J., 2017. Relationships between the potential production of the greenhouse gases CO_2, CH_4 and N_2O and soil concentrations of C, N and P across 26 paddy fields in southeastern China. Atmos. Environ. 164, 458-467. http://dx.doi.org/10.1016/j.atmosenv.2017.06.023

Yang, P., Tang, K.W., Tong, C., Lai, D.Y.F., Zhang, L.H., Lin, X., Yang, H., Tan, L.S., Zhang, Y.F., Hong, Y., Tang, C., Lin, Y.X. 2022a. Conversion of coastal wetland to aquaculture ponds decreased N_2O emission: Evidence from a multi-year field study. Water Res. 227, 119326. https://doi.org/10.1016/j.watres.2022.119326

Yang, P., Tang, K.W., Tong, C., Lai, D.Y.F., Wu, L., Yang, H., Zhang, L., Tang, C., Hong, Y., Zhao, G., 2022b. Changes in sediment methanogenic archaea community structure and methane production potential following conversion of coastal marsh to aquaculture ponds. Environ. Pollut. 305, 119276. https://doi.org/10.1016/j.envpol.2022.119276

Author Contribution Statement

Conceptualization: Lishan Tan, Ping Yang, Chuan Tong, Kam W. Tang

Methodology: Lishan Tan, Ping Yang, Kam W. Tang, Manjing Ruan

Formal analysis: Lishan Tan, Linhai Zhang, Ping Yang, Kam W. Tang, Manjing Ruan

Validation: Ping Yang, Kam W. Tang

Investigation: Lishan Tan, Linhai Zhang, Ping Yang, Yan Hong, Yalan Tian, Chen Tang

Data Curation: Lishan Tan, Linhai Zhang, Ping Yang

Writing-Original Draft: Lishan Tan, Ping Yang

Writing - Review & Editing: Chuan Tong, Derrick Y. F. Lai, Hong Yang, Kam W. Tang

Project Administration: Ping Yang, Chuan Tong

Funding acquisition: Ping Yang, Chuan Tong